# Higher performance enhancement of direct torque control by using Space Vector Modulation for doubly fed induction machine

*Radouan Gouaamar*[1*], *Adiba EL Fadl*[1], *Seddik Bri*[1], and *Zineb Mekrini*[2]

[1]Materials and Instrumentation (MIM), High School of Technology, Moulay Ismail University, Meknes, Morocco.
[2]Iindustrial Systems Engineering and Energy Conversion Team, FSTT, Abdelmalek Essaadi University, Tetouan, Morocco.

**Abstract.** This research work aims at current literature review and extensive performance improvement in Direct Torque Control using Space Vector Modulation (DTC-SVM) by considering Doubly Fed Induction Machines. In order to determine the effectiveness of DFIM, significant focus needs to be placed on its speed control design. For highly perturbed systems, traditional Proportional-Integral (PI) speed controllers fail as their gain values are a function of system parameters that inherently change such as engine properties. Therefore, a strong speed controller is necessary to realize high-performance drives. To overcome these confrontations, the proposed study presents backstepping speed control which performs better in terms of accuracy of speed, dynamic tracking and robustness against load disturbances. All proposed control algorithms have been subjected to rigorous tests and simulations using a MATLAB/Simulink environment. A comprehensive study comparing the performance of these speed control within DTC framework is carried out with a detailed insight to important metrics such as dynamic response, reference tracking, torque ripple content involved and complexity among others. This study discusses the pros and cons of all mentioned methods, which helps in better understanding for optimal speed control selection to improve DFIM performance at different operating conditions. The results of this research should help in the further development of control strategies for electric machines to make them more efficient and reliable when used.

**Keywords:** Direct torque control, backstepping controller, doubly fed induction machine, Space Vector Modulation, proportional-integral controller.

## 1 Introduction

* Corresponding author: radouan.gouaamar@gmail.com

Electric machines are integral to numerous industrial processes, with their performance requirements varying widely depending on the application. Doubly Fed Induction Machines (DFIMs) are particularly favored for their high efficiency, power quality, reliability, and longevity [1]. DFIMs are widely utilized in traction systems, marine propulsion, electric and hybrid cars, and wind and hydroelectric power generation as variable speed generators. Despite these advantages, DFIMs pose several challenges [2]:

- Complex dynamic behavior
- Equations that are extremely coupled, multivariate, and nonlinear
- State variables that are not readily quantifiable, such as flux

To address these challenges, robust control techniques have been developed. Since its introduction in the 1970s, Field-Oriented Control (FOC) has offered fast torque response and excellent efficiency across a broad speed range by providing decoupling between electromagnetic torque and flux [3]. However, FOC is complex and sensitive to parametric variations. Direct Torque Control (DTC), developed by Takahashi in the early 1980s, simplifies this by eliminating the need for current regulation and coordinate transformation [4]. The incorporation of Space Vector Modulation (SVM) into DTC (DTC-SVM) has attracted a great deal of attention because of its dynamic responsiveness, straightforward design, and low reliance on machine parameters [5].

In order to monitor flux and electromagnetic torque, DTC-SVM uses hysteresis regulators and switching tables. A Proportional-Integral (PI) controller is used in the outer loop to manage speed. However, PI controllers are less effective under system disturbances and their gain values vary with machine parameters. To achieve high-performance drives, a robust speed control is necessary. By using reliable and efficient speed controllers, this research seeks to improve DTC performance for DFIMs [6].

The development of a backstepping speed regulator enables constant torque and motor speed control. Utilizing the Lyapunov stability function, this nonlinear-to-linear system transformation provides resilience against load disturbances, high performance, speed accuracy, and dynamic tracking behavior. A comparative analysis of this backstepping controller against traditional PI controllers within the DTC framework is conducted to evaluate their effectiveness [7].

The structure of this paper is as follows: Section 2 presents the dynamic model of the DFIM. Section 3 discusses the classical DTC-SVM technique. Section 4 designs three speed regulators for the DTC-SVM strategy. Simulation results using MATLAB/SIMULINK are presented and interpreted in Section 5.The final section concludes the paper and offers recommendations for future work.

## 2 Model of the Doubly Fed Induction Machine

The two-phases model is the best choice for analyzing the dynamic properties and for creating and applying DTC-SVM on the DFIM. Equations (1, 2, 3) appropriately characterize this model in the (α, β) frame [8].

Electrical equations:

$$V_{S_{\alpha,\beta}} = R_s . i_{s_{\alpha,\beta}} + \frac{d\varphi_{s_{\alpha,\beta}}}{dt} \tag{1}$$

$$V_{r_{\alpha,\beta}} = R_r . i_{r_{\alpha,\beta}} + \frac{d\varphi_{r_{\alpha,\beta}}}{dt} \pm \omega_m . \varphi_{r_{\alpha,\beta}} \tag{2}$$

Magnetic equations:

$$\varphi_{s_{\alpha,\beta}} = L_s.\, i_{s_{\alpha,\beta}} + L_m.\, i_{r_{\alpha,\beta}} \tag{3}$$

$$\varphi_{r_{\alpha,\beta}} = L_r.\, i_{r_{\alpha,\beta}} + L_m.\, i_{s_{\alpha,\beta}} \tag{4}$$

Mechanical equations:

$$T_{em} = P\left(\varphi_{s_\alpha} i_{s_\beta} - \varphi_{s_\beta} i_{s_\alpha}\right) \tag{5}$$

$$J.\frac{d\Omega}{dt} + f.\omega = T_{em} - T_r \tag{6}$$

## 3 Direct torque control based on space vector modulation

The two main problems with conventional DTC are variable switching frequency and high ripples. These problems cause unwanted consequences like higher current harmonics, noise pollution, and poor control performance, particularly at low speeds. The width of the hysteresis band determines how big the ripples are. Worse, because hysteresis controllers are discrete, the ripples still matter even at narrower bandwidth values. Moreover, very small bandwidth values cause the inverter's switching frequency to increase.
To get over these problems, torque, stator flux, and rotor flux are controlled by DTC-SVM for DFIM control using three Proportional-Integral (PI) controllers and two inverters. The torque PI controller produces the quadratic rotor and stator voltages, whereas the output of the other two PI controllers in the flux loop produces the direct voltages. After obtaining Vd and Vq, they must be converted into a fixed reference (α, β) in order to be used as an input by the space vector modulator (SVM). For the inverters' power transistors, the SVM delivers switching signals (SA, SB, and SC) [9].

### 3.1 Estimation of the torque electromagnetic and flux

The Doubly Fed Induction Machines current and voltage measurements are used to evaluate the rotor and stator flux vectors' amplitude and location. In the reference frame (α, β), the stator and rotor flow vectors are expressed as follows [10]:

$$\hat{\varphi}_{s_{\alpha,\beta}} = \int_0^t \left(v_{s_{\alpha,\beta}} - R_s.\, i_{s_{\alpha,\beta}}\right) dt \tag{7}$$

$$\hat{\varphi}_{r_{\alpha,\beta}} = \int_0^t \left(v_{r_{\alpha,\beta}} - R_r.\, i_{r_{\alpha,\beta}}\right) dt \tag{8}$$

With $\bar{\varphi}_{s,r} = \hat{\varphi}_{(s,r)_\alpha} + j.\hat{\varphi}_{(s,r)_\beta}$

The amplitude of the flux vectors in the rotor and stator may be represented as follows:

$$\hat{\varphi}_{s,r} = \sqrt{\hat{\varphi}^2_{(s,r)_\alpha} + \hat{\varphi}^2_{(s,r)_\beta}} \tag{9}$$

The locations of the flux vectors are found using the formula below:

$$\theta_{s,r} = \tan^{-1} \frac{\hat{\varphi}_{(s,r)_\beta}}{\hat{\varphi}_{(s,r)_\alpha}} \tag{10}$$

The electromagnetic torque is calculated using the measured stator currents:

$$\hat{T}_{em} = P\left(\hat{\varphi}_{s_\alpha} i_{s_\beta} - \hat{\varphi}_{s_\beta} i_{s_\alpha}\right) \tag{11}$$

### *3.1.1 DTC-SVM control applied to the DFIM*

Compared to traditional pulsewidth modulation (PWM), the SVM is distinct. Its foundation is the inverter output's vectorial spatial representation. Every phase does not have its own modulator. The voltage vector's components in the complex plane, or the spatial voltage vector, supply the reference voltages. By projecting the reference vector Vref across adjacent vectors that correspond to two non-zero switching states, the SVM idea predicts the inverter voltage vector. The switching vector diagram of a two-level inverter, as seen in Fig. 1, yields a hexagon with six sectors, each of which is 60° stretched [11] [12].

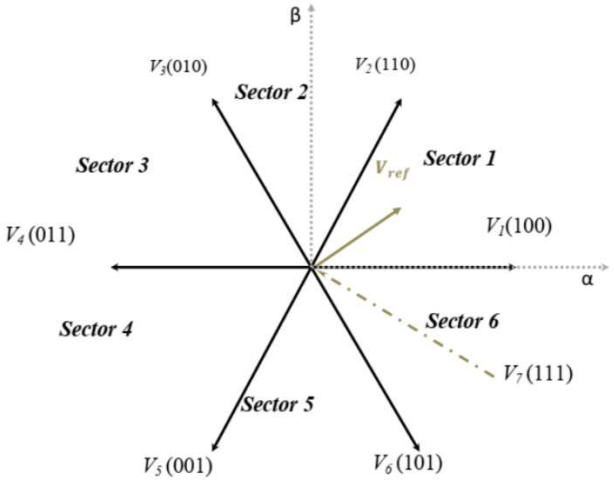


**Fig. 1.** Voltage space vector diagram.

Vector calculations can be used to determine how long each vector will take to apply; the zero vector will be applied for the remaining time. When the reference voltage is in sector 1 (Fig. 2), it may be synthesized using the vectors V1, V2, and V0 (zero vector). The following is an expression of the sector 1 volt-second principle:

$$V_{ref}.T_e = V_1.T_1 + V_2.T_2 + V_0.T_0 \tag{12}$$

$$T_e = T_1 + T_2 + T_0 \tag{13}$$

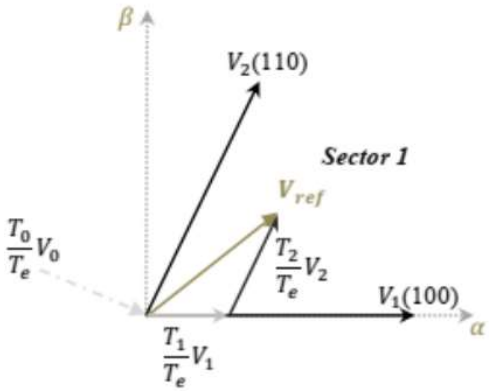


**Fig. 2.** Reference vector at sector 1 as a composite of nearby vectors.

The voltage vectors' corresponding application times are T0, T1, and T2. Simple projections are used to determine the timings $T1$ and $T2$, which correspond to the voltage vectors:

$$T_1 = \frac{T_e}{2V_{dc}}\left(\sqrt{6}V_\beta - \sqrt{2}V_\alpha\right) \tag{14}$$

$$T_2 = \frac{T_e}{V_{dc}}.\sqrt{2}V_\alpha \tag{15}$$

For the sectors, the previously described approach for Vref between V1 and V2 is repeated. Table 1 displays the various state vector application times for the various sectors (S1 through S6) based on the values of the variables X, Y, and Z: Alongside:

$$X = \frac{T_e}{V_{dc}}.\sqrt{2}V_\alpha \tag{16}$$

$$Y = \frac{T_e}{2V_{dc}}\left(\sqrt{6}V_\beta + \sqrt{2}V_\alpha\right) \tag{17}$$

$$Z = \frac{T_e}{2V_{dc}}\left(-\sqrt{6}V_\beta + \sqrt{2}V_\alpha\right) \tag{18}$$

**Table 1.** Inverter switch control signals.

| Sector 1 | Sector 2 | Sector 3 | Sector 4 | Sector 5 | Sector 6 |
|---|---|---|---|---|---|
| $\boldsymbol{T_1 = -Z, T_2 = X}$ | $T_2 = Y, T_3 = Z$ | $T_3 = X, T_4 = -Y$ | $T_4 = Z, T_5 = -X$ | $T_5 = -Y, T_6 = -Z$ | $T_6 = -X, T_1 = Y$ |

The following is the expression used to calculate the duty cycles (or switching times):

$$T_{aon} = \frac{T_e - T_1 - T_2}{2} \tag{19}$$

$$T_{bon} = T_{aon} + T_1 \tag{20}$$

$$T_{con} = T_{bon} + T_2 \tag{21}$$

The SVM model produces a symmetric carrier wave. An example of this wave with a period of $Te$ in sector 1 is seen in Fig. 3. The overall layout of the DTCSVM control for the doubly fed induction machine coupled by two voltage inverters is shown in Fig. 4.

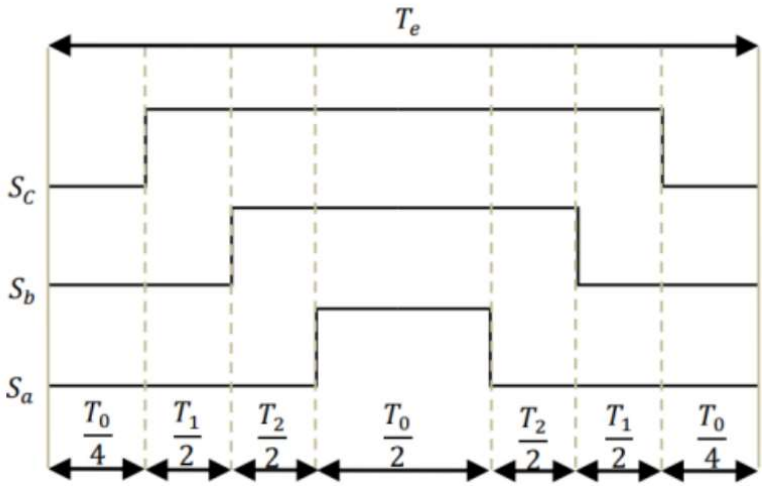


**Fig. 3.** Switching times of sector 1.

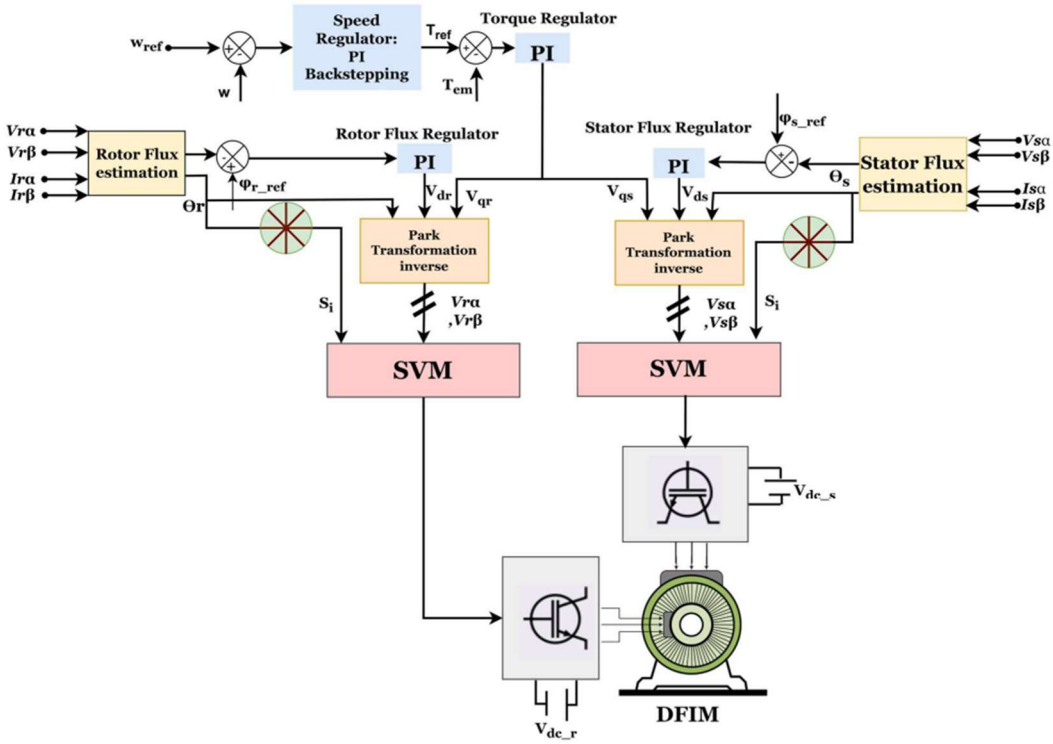


**Fig. 4.** Block Diagram for DFIM Drive's DTC-SVM Scheme.

## 4 Speed Controllers

### 4.1 PI controller

To guarantee superior tracking and optimal performance, the rotation speed control is necessary. In this section, two different kinds of speed control are covered.

Integral-proportional controller Machine drives are controlled by the proportional-integral (PI) regulator (PI) due to its many benefits. It is, in fact, easy to use, quick to deploy, and capable of producing passable results. We are interested in studying the speed restriction system because of this. The typical PI speed controller needs a precise mathematical description of the system and the right gain values in order to provide an efficient drive [13].

$$T_{em} = \left(k_p + \frac{k_i}{s}\right).\varepsilon_\Omega \tag{22}$$

### 4.2 Backstepping controller

Through the application of Lyapunov's theorem, this method seeks to linearize a nonlinear system. For assessing the stability of dynamic systems, it is an effective method.Through speed regulation of DFIMs, this control method enhances robustness and performance [13]:

$$\frac{d\omega}{dt} = \frac{1}{J}[T_{em} - T_L - f.\omega] \quad (23)$$

Where: Determining the speed mistake is the first stage in the backstepping control process.

$$\varepsilon(t) = \omega_{ref}(t) - \omega(t) \quad (24)$$

After that, the speed error derivative may be shown as:

$$\dot{\varepsilon}(t) = \dot{\omega}_{ref}(t) - \dot{\omega}(t) \quad (25)$$

Then:

$$\dot{\varepsilon}(t) = \dot{\omega}_{ref}(t) - \frac{1}{J}.T_{em} + \frac{1}{J}.T_L + \frac{f}{J}.\omega \quad (26)$$

Consequently, the following definition of the Lyapunov function applies:

$$v(t) = \frac{1}{2}\varepsilon^2(t) \quad (27)$$

Thus, its derivative is:

$$\dot{v}(t) = \varepsilon(t).\dot{\varepsilon}(t) = \varepsilon(t)\left[\dot{\omega}_{ref}(t) - \frac{1}{J}.T_{em} + \frac{1}{J}.T_L + \frac{f}{J}.\omega\right] \quad (28)$$

Finding System Stability: Using Negative Lyapunov Function Derivatives to Their Full Potential. A critical step in guaranteeing the stability of the system is to derive a negative derivative of the Lyapunov function. The derivative is represented by equation (29), which is completed by adding a positive constant.

$$\dot{v}(t) = -K\varepsilon^2(t) \leq 0 \quad (29)$$

## 5 Simulation Results

The results of the simulation are shown in the following figures:
The machine's rotation speed and electromagnetic torque are shown to follow their references in Figs. 5 and 6. The backstepping DTC-SVM control has a faster rise time than the PI DTC-SVM control, with a speed response time of around 1.4 ms. Furthermore, it is clear that neither control technique's system speed response is impacted by the impacts of load torque.

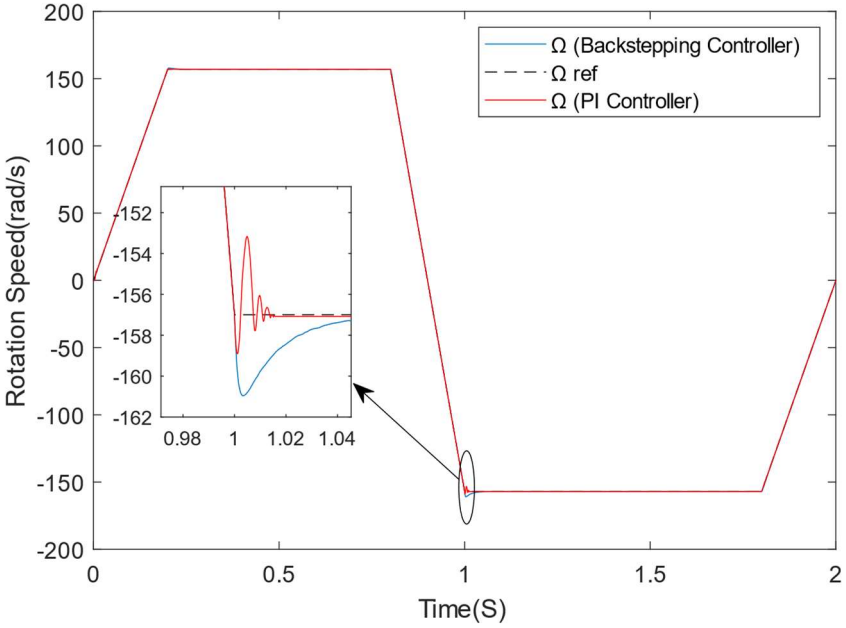


**Fig. 5.** Rotation speed.

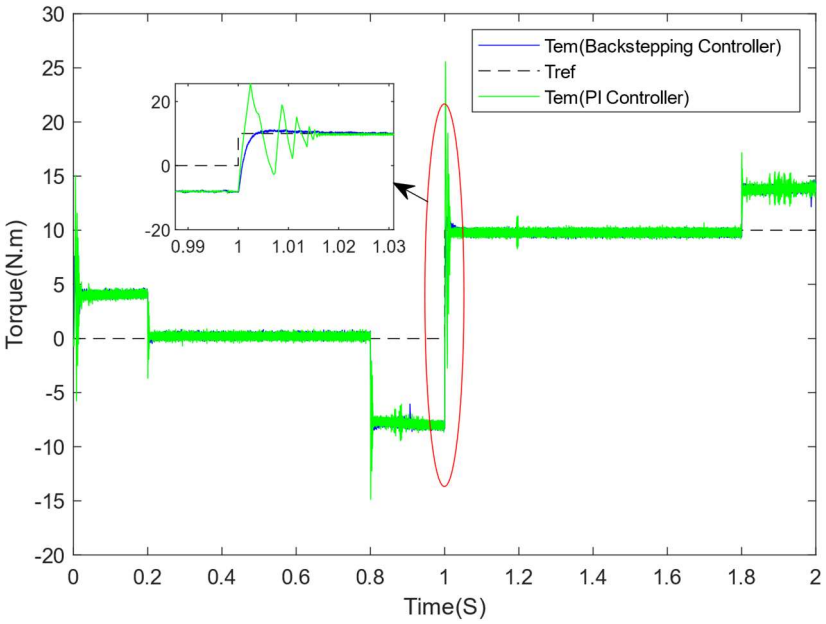


**Fig. 6.** Electromagnetic torque.

The modulus of the rotor and stator flux vectors, as shown in Figs. 7 and 8, exactly matches the reference flux (0.5Wb for the rotor flux and 1Wb for the stator flux).

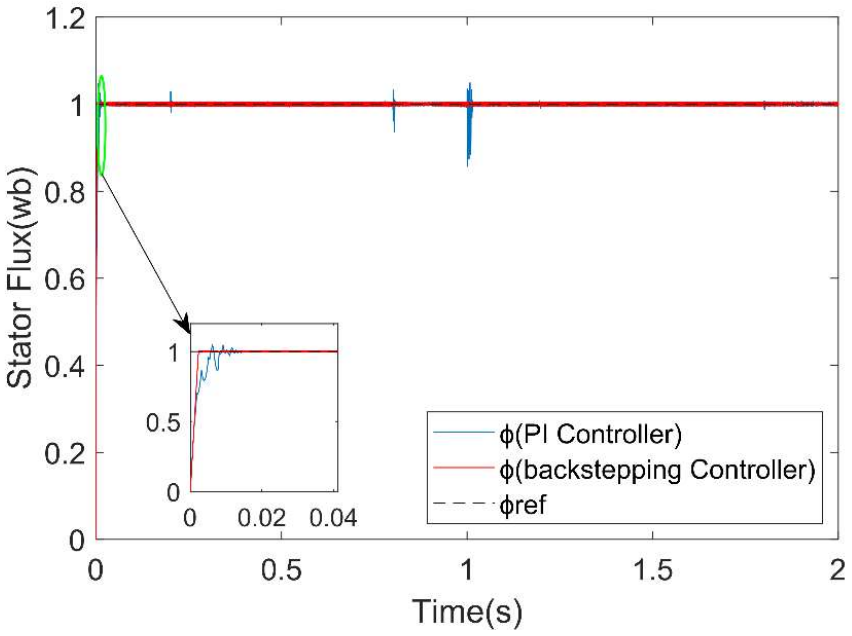


**Fig. 7.** Stator flux.

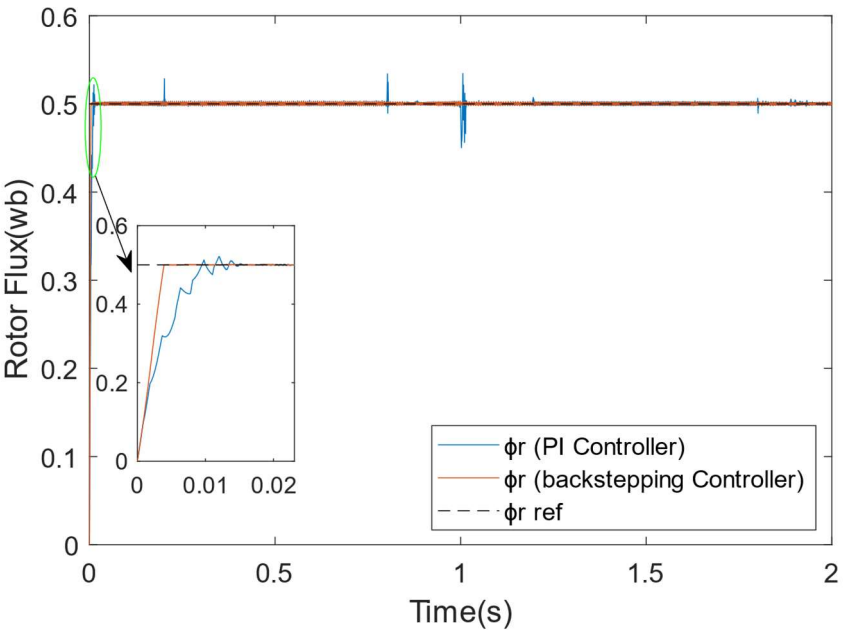


**Fig. 8.** Rotor flux.

When using a the backstepping DTC-SVM, the machine's electromagnetic torque and flux oscillate less than when using PI DTC-SVM control. Comparing this trajectory to that produced by the traditional DTC, the rotor and stator flux have a finer circular shape (Fig.

9). Furthermore, it is seen that variations in the torque have no effect on the flux, indicating a decoupling of the flux and the torque. These findings demonstrate the backstepping DTC-SVM control's resilience and what appears to be a decrease in the ripples caused by flux and torque.

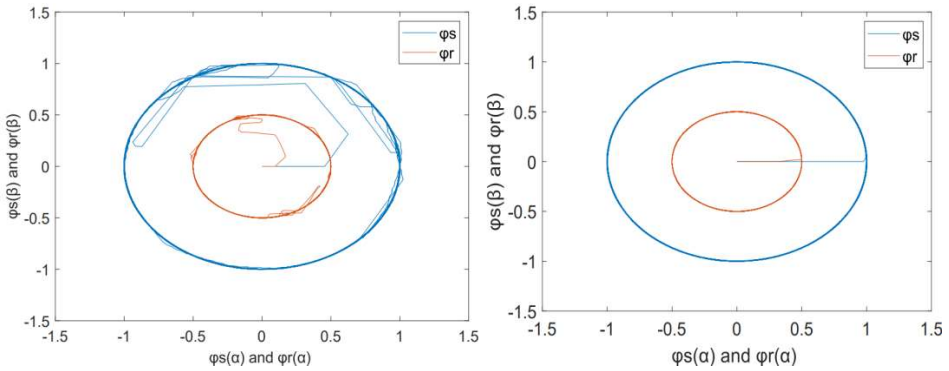


**Fig. 9.** Evolution of the rotor and stator flux by the control: (a) PI DTC-SVM (b) backstepping DTC-SVM.

Figures 10, 11, 12, and 13 depict the stator (isa,isb,and isc) and rotor current components (ira,irb, and irc)in the frame, respectively. These currents exhibit sinusoidal patterns with frequencies corresponding to the reference speed in response to fluctuations imposed by the torque of the load.

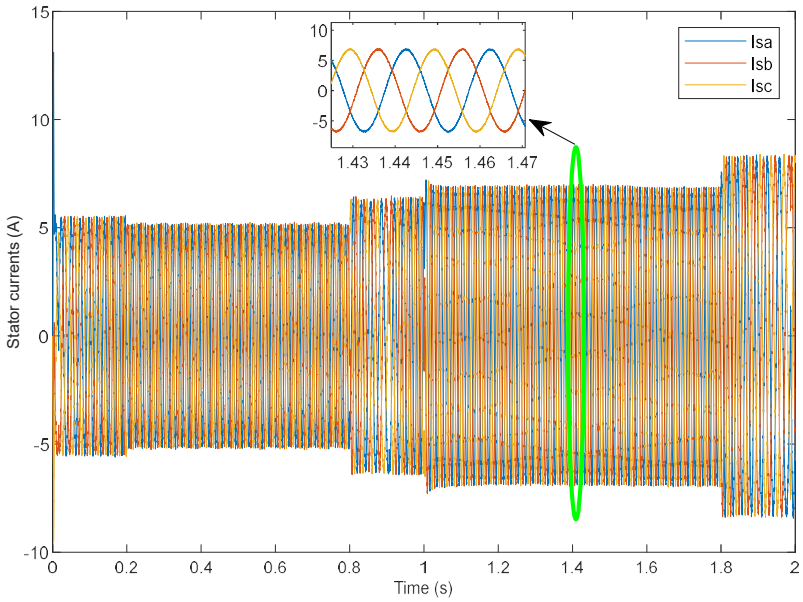


**Fig. 10.** Stator currents by backstepping DTC-SVM control.

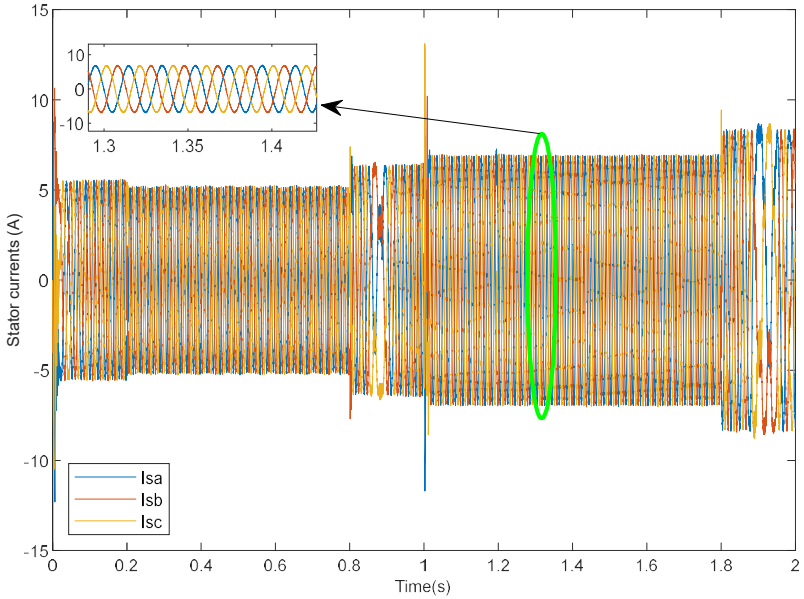


**Fig. 11.** Stator currents by PI DTC-SVM control.

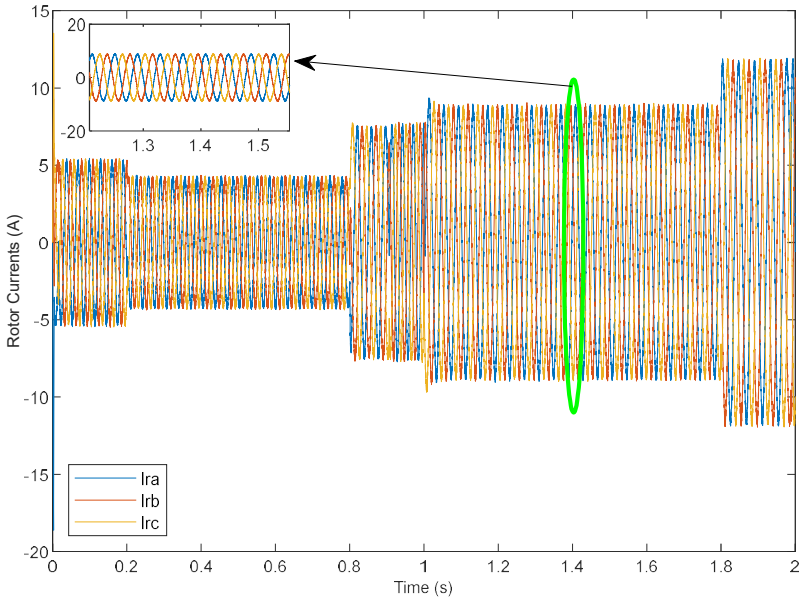


**Fig. 12.** Rotor currents by backstepping DTC-SVM control.

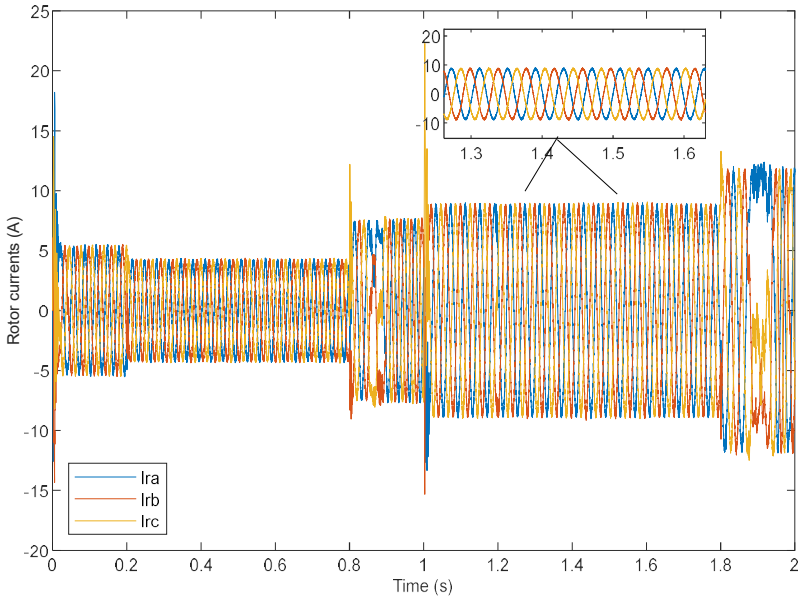


**Fig. 13.** Rotor currents by PI DTC-SVM control.

Figures 14 and 15 show the Total Harmonic Distortion profiles related to the stator phase "b" and the absorbed rotor current of the Doubly Fed Induction Motor (DFIM). The results clearly show that a significant decrease in the THD of the currents may be obtained by using the backstepping DTC-SVM control instead of the PI DTC-SVM.

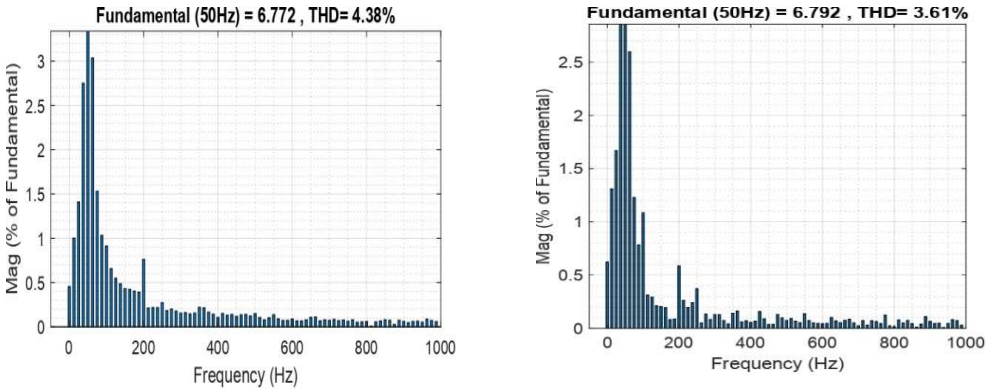


(a) (b)

**Fig. 14.** THD of stator current by: (a) PI DTC-SVM (b) backstepping DTC-SVM.

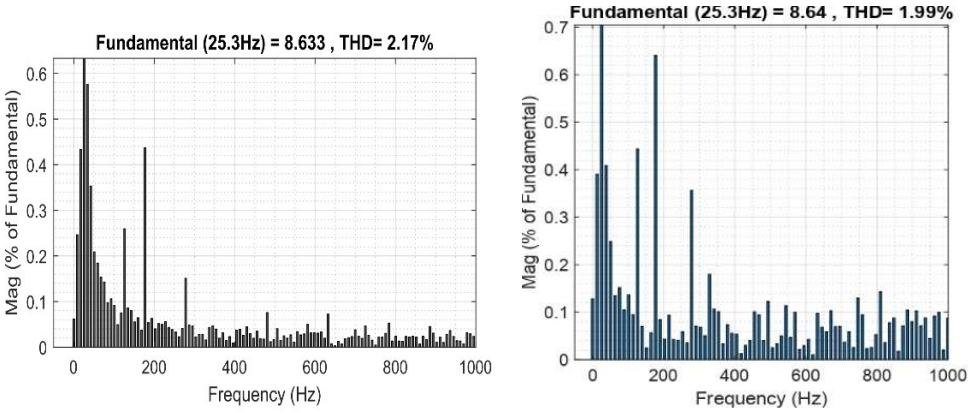


(a) (b)

**Fig. 15.** THD of stator current by: (a) PI DTC-SVM versus (b) Backstepping DTC-SVM.

The results show that the best torque and flux control increases output power quality and maximizes THD. It is well known that changes in torque and flux significantly affect the currents' total harmonic distortion (THD). A notable reduction in THD is obtained when comparing the PI DTC-SVM with the backstepping DTC-SVM.

Table 2 presents a concise overview encompassing rising time, torque ripples, flux ripples in the stator and rotor, as well as a comprehensive current harmonic analysis, drawing a comparison between the PI DTC-SVM and the backstepping DTC-SVM. This table serves as a testament to the numerous merits offered by the backstepping DTC-SVM approach, including optimized rising time, substantial mitigation of torque and flux ripples, as well as a notable reduction in stator and rotor current harmonics. Consequently, the recommended method surpasses the performance of the PI DTC-SVM strategy.

**Table 2.** Comparative Results: PI DTC-SVM vs. Backstepping DTC-SVM are revealed.

| Performance | PI DTC-SVM | backstepping DTC-SVM |
|---|---|---|
| **Rise time of the speed (ms)** | 2.16 | 1.4 |
| **Torque ripple (N.m)** | 3.06 | 2.0321 |
| **Stator flux ripple (Wb)** | 0.0543 | 0.0367 |
| **Rotor flux ripple (Wb)** | 0.076 | 0.052 |
| **THD of staor current isb (%)** | 4.38 | 3.61 |
| **THD of rotor current irb (%)** | 2.17 | 1.99 |

Table 3 Comparison of the proposed method to several other documented control strategies It is important to note that these methodologies are not technically compared under the same conditions, as very few works were implemented in similar contexts. Consequently, as the comparison results in our paper and using sliding mode [14], it can be assured that less torque fluctuation of our proposed solution. Moreover, Our system is even impervious to load torque variations which further illustrates its robustness. Compared with the DTC applying RTOA-DTC showed in [15], it also has a propensity for more torque oscillations, but both amiably complex control mechanisms. The necessity of these fast processors adds complexity and in some cases, higher system costs.

**Table 3.** Comparative Evaluation: Our Approach Versus Selected Control Strategies from Literature.

| **References of Publications** | Proposed technique | [14] | [15] |
|---|---|---|---|
| **Techniques** | backstepping DTC SVM | SMC | RTOA-DTC |
| **Torque Ripples Amplitude (Nm)** | 2.0321 | 2.4 | 12 |
| **Speed Response Time (s)** | 1.4 | 0.19 | 0.1561 |
| **Robustness** | Robust | Robust | Robust |

## 6 Conclusion

In this study, we suggest a novel backstepping direct torque control system for a dual voltage source inverter-powered DFIM. Improving DTC-SVM's performance is the main goal of this work. We show the DFIM modeling and offer thorough explanations of the DTC-SVM approach. In particular, we provide a thorough control plan using backstepping controllers.
We used MATLAB/SIMULINK to perform system control tests in order to assess the efficacy of the suggested plan. The following are the main conclusions of our work:

- Reducing torque and flux ripples allows the backstepping controller to effectively enhance DTC-SVM performance. As a result, issues like temperature, mechanical vibration, and aging are less frequent for the motor.

- Our method maintains the traditional DTC-SVM's rapid reaction time and resilience.

- Improved harmonic distortion in stator and rotor currents is a result of the backstepping controller's capacity to adjust torque and flux.

Our next research endeavors will center on testing the suggested approach in experiments. Furthermore, our goal is to create a hybrid model that combines many techniques to enhance the control approach that we have examined in this study.

## References

1. Ghamri, A., Boumaaraf, R., Benchouia, M. T., Mesloub, H., Goléa, A., & Goléa, N. (2020). Comparative study of ANN DTC and conventional DTC controlled PMSM motor. Mathematics and Computers in Simulation, 167, 219–230.
2. Iwa ´nski, G.; Piwek, M.; Dauksha, G. Doubly Fed Induction Machine-Based DC Voltage Generator with Reduced Oscillations of Torque and Output Voltage. Energies 2023, 16, 814. https:// doi.org/10.3390/en16020814.
3. Sabir, O.: Robust DPC-SVM control strategy for shunt active power filter based on H∞ regulators. Int. J. Electr. Power Energy Syst. 117, 105699 (2020)
4. Blaschke, F.: The principle of field orientation as applied to the new TRANSVECTOR closed loop control system for rotating field machines. Siemens Rev. 34(5), 217–220 (1972)
5. Giribabu D, Srivastava SP, Pathak MK (2019) Modified reference model for rotor flux-based MRAS speed observer using neural network controller. IETE J Res 65(1):80–95.
6. Guven, S., Usta, M. A., & Okumus, H. I. (2018). An improved sensorless DTC-SVM for three-level inverter-fed permanent magnet synchronous motor drive. Electrical Engineering, 100(4), 2553–2567.

7. Gouaamar, Radouan & Bri, Seddik & Mekrini, Zineb & Oufettoul, Hicham. (2024). Advancing Wind Energy: Implementation of a Robust Nonlinear Control for DFIG Turbines. 10.1007/978-3-031-68660-3_45.
8. Zhao, J.; Xi, M. Self-Tuning of PID Parameters Based on Adaptive Genetic Algorithm. IOP Conf. Ser. Mater. Sci. Eng. 2020, 782, 042028.
9. Baala, Youssef and Seddik Bri. "DFIG-Based Wind Turbine Robust Control: Using High-Order Sliding Mode and a Kalman Observer." Proceedings of the 4th International Conference on Big Data and Internet of Things (2019): n. pag.
10. Gouaamar, Radouan, Seddik Bri and Zineb Mekrini. "Comparative Analysis between Proportional-Integral and Artificial Neural Network Control of a Grid-Connected PV System." E3S Web of Conferences,n. pag.2023.
11. B. L. G. Costa, C. L. Graciola, B. A. Angélico, A. Goedtel, and M. F. Castoldi, "Metaheuristics optimization applied to PI controllers tuning of a DTC-SVM drive for three-phase induction motors", Applied Soft Computing, Vol. 62, pp. 776-788, 2018.
12. R. Gouaamar, S. Bri and Z. Mekrini. "Improvements the direct torque control performance for an induction machine using fuzzy logic controller." International Journal of Electrical and Computer Engineering (IJECE), Vol. 14, No. 1, pp.1-11, February 2024.
13. Schockenhoff, F.; Zähringer, M.; Brönner, M.; Lienkamp, M. Combining a Genetic Algorithm and a Fuzzy System to Optimize User Centricity in Autonomous Vehicle Concept Development. Systems 2021, 9, 25.
14. Abderazak, S.; Farid, N. Comparative study between Sliding mode controller and Fuzzy Sliding mode controller in a speed control for doubly fed induction motor. In Proceedings of the 2016 4th International Conference on Control Engineering & Information Technology (CEIT), Hammamet, Tunisia, 16–18 December 2016; pp. 1–6.
15. Nsugbe, E.; Connelly, S. Multiscale depth of anaesthesia prediction for surgery using frontal cortex electroencephalography. Healthc. Technol. Lett. 2022, 9, 43–53.